Climate Change Sensitivity Study of California Hydrology
A Report to the California Energy Commission

LBNL Technical Report No. 49110
November 2001

Norman L. Miller and Kathy E. Bashford
California Water Resources Research and Applications Center
Lawrence Berkeley National Laboratory, University of California

and

Eric Strem
California-Nevada River Forecast Center
NOAA-National Weather Service

ABSTRACT

Recent reports based on climate change scenarios have suggested that California will be subjected to increased wintertime and decreased summertime streamflow. Due to the uncertainty of projections in future climate, a range of potential climatological future temperature shifts and precipitation ratios is applied to the Sacramento Soil Moisture Accounting Model and Anderson Snow Model in order to determine hydrologic sensitivities. Two GCM projections were used in this analysis: one that is warm and wet (HadCM2 run 1) and one that is cool and dry (PCM run B06.06), relative to the GCM projections that were part of the Third Assessment Report of the Intergovernmental Panel on Climate Change. An additional set of specified incremental temperature shifts (1.5 ^{o}C, 3.0 ^{o}C, and 5.0 ^{o}C) and precipitation ratios (1.00, 1.09, 1.18, and 1.30) were also used as input to the snow and soil moisture accounting models. Calculations were performed for a set of California river basins that extend from the coastal mountains and Sierra Nevada northern region to the southern Sierra Nevada region. Results from this study indicate that for all cases, a larger proportion of the streamflow volume will occur earlier in the year. The amount and timing is dependent on the characteristics of each basin, particularly the elevation of the freezing line. The hydrologic response varies for each scenario and the resulting solution set provides bounds to the range of possible change in streamflow, snowmelt, snow water equivalent, and the change in the magnitude of annual high flow days.

INTRODUCTION

The Intergovernmental Panel on Climate Change (IPCC) Third Assessment Report (IPCC TAR 2001) and the U.S. Global Climate Change Research Program (USGCRP) Report of the Water Sector (Water 2001) summarize potential consequences due to global warming. The IPCC reports that climate model projections with a transient one percent annual increase in greenhouse gas emissions show an increase in the global mean near-surface air temperature by 1.4 to 5.8 ^{o}C, with a 95% probability interval of 1.7 to 4.9 ^{o}C by 2100 (Wigley and Raper 2001). Both reports indicate that likely changes during the 21st century include: higher maximum and minimum temperatures with a decreasing diurnal range over U.S. land areas, more intense precipitation events, increased summer continental drying, and increased risk of drought. To assess the impacts on water resources, hydrologic simulations based on climate model projections and specified incremental temperature and precipitation changes that bracket the range of possible outcomes are necessary.

There have been a number of investigations of California hydrologic response focused on changes in streamflow volumes due to climate change (e.g. Revelle and Waggoner 1983, Gleick 1987, Lettenmaier and Gan 1990, Jeton et al. 1996, Miller et al. 1999, Wilby and Dettinger 2000, Knowles and Cayan 2001). Revelle and Waggoner (1983) developed regression models to estimate the sensitivity of streamflow in major basins to climate change from historical data. Gleick (1987) used a modified upper and lower basin water budget model (Thornwaite 1948) for the Sacramento drainage directly forced by precipitation and temperature output from three GCMs. Lettenmaier and Gan (1990) used precipitation and temperature from three GCM scenarios to force process-based basin-scale water budget models (Burnash et al. 1973; Anderson 1973) with three to five elevation band defined subbasins, at four basins (North Fork American, Merced, McCloud, Thomes Creek) in the Sacramento-San Joaquin drainage. Jeton et al. (1996) ran a distributed parameter precipitation runoff model (Leavesley et al. 1983) to evaluate the North Fork American and East Fork Carson Rivers using specified incremental temperature and precipitation as uniform climate change scenarios. Miller et al. (1999) dynamically downscaled a GCM projection via a regional climate model and used the output as forcing to process based hydrologic models (Beven and Kirkby 1979, Leavesley et al. 1983) in the North Fork American River and the north coastal Russian River. Knowles and Cayan (2001) used historical precipitation and a single GCM projection of temperature that was statistically interpolated to a 4 km resolution as input forcing to a modified version of the Burnash et al. (1973) soil moisture accounting model (Knowles 2000) for the entire Sacramento-San Joaquin drainage.

In general, each of these studies has suggested that Sierra Nevada snowmelt driven streamflows are likely to peak earlier in the season under global warming due to increased atmospheric green house gas (GHG) concentrations. A key finding of these studies is that one of the greatest influences on streamflow sensitivity to climate change is the basin elevation and where the freezing line is located. To further understand the likelihood of potential shifts in the timing and magnitude of California streamflow, and related hydrologic response, the following study analyzes six major watersheds forced by two end-member GCM projections and by specified incremental temperature (shifts) and precipitation (ratios) changes.

APPROACH

The focus of this study is to determine the range of the effects of projected climate change scenarios for assessing California water resources. Streamflow sensitivities for the watersheds studied were related to a larger set of watersheds representing the entire Sacramento-San Joaquin drainage and will be applied to water demand and allocation simulations.

Streamflow simulations in this study are based on the application of the National Weather Service - River Forecast System (NWSRFS) Sacramento Soil Moisture Accounting (SAC-SMA) Model (Burnash et al. 1973) coupled to the snow accumulation and ablation Anderson Snow Model (Anderson 1973). The SAC-SMA has two upper zone storage compartments (free and tension) and three lower zone storage compartments (free primary, free secondary, and tension). Tension zone storage is depleted only by evapotranspiration processes, while the free zone water drains out as interflow and baseflow. The SAC-SMA was chosen primarily due to its dependence on only two variables, precipitation and temperature, and because it is the operational model of the National Weather Service. It has been used in previous climate change sensitivity studies (Lettenmaier and Gan 1990, Miller et al. 2000) with an assumption of geomorphologic stream channel stationarity. Assuming fixed channel geometry requires that climate change simulations be based on perturbations about the historical data period for which the calibration was performed and verified (Lettenmaier and Gan 1990). Historical temperature and precipitation time series for 30 years (1963-1992) is sufficiently long for a representative climatology and is available at 6-hour time steps for each basin. The snow producing basins were delineated into upper and lower basins with separate input forcing to account for the elevation, land surface characteristics, and climate differences.

Six representative headwater basins (Smith River at Jed Smith SP, Sacramento River at Delta, Feather River at Oroville Dam, American River at North Fork Dam, Merced River at Pohono Bridge, and Kings River at Pine Flat Dam) with natural flow were selected for analysis in this study (Figure 1.). Table 1 shows the basin size, location, percent area, and the centroid of each upper and lower subbasin. The Smith is a very wet coastal basin that does not significantly accumulate seasonal snowpack. The Sacramento is a mountainous northern California basin with a small amount of seasonal snow accumulation. The Sacramento provides streamflow for the north and northwest drainage region into the Central Valley. The Feather and the Kings represent the northernmost and southernmost Sierra Nevada basins for this study, and the Kings and Merced are the highest elevation basins. The American is a fairly low elevation Sierra Nevada basin, but has frequently exceeded flood stage, resulting in substantial financial losses. This set of study basins provides sufficient information for a spatial estimate of the overall response of California's water supply (excluding the Colorado River) and will help to give an indication of the potential range of impacts.

	Smith	Sacramento	Feather	American	Merced	Kings
Area sq. km	1706	1181	9989	950	891	4292
Gage Lat.	41º 47' 30"	40º 45' 23"	39º 32' 00"	38º 56' 10"	37º 49' 55"	36º 49' 55"
Gage Lon.	124º 04'30"	122º 24' 58"	121º 31' 00"	121º 01' 22"	119º 19' 25"	119º 19' 25"
Percent Upper	0	27	58	37	89	72
Upper Centroid		1798	1768	1896	2591	2743
Lower Centroid	722	1036	1280	960	1676	1067

Table 1. Basin Area, stream gauge coordinates, percent subbasin area and elevation.

Historical precipitation and temperature input forcing to the hydrologic models are based on the archived NWS 6-hour mean area precipitation (MAP) and mean area temperature (MAT) for each upper and lower basin. Historical daily streamflow was also provided by the NWS for the stream gages at the outlet of each of the six basins.

Figure 1. Location of the six study basins (Smith-at Jed Smith, Sacramento at Delta, Feather at Oroville Dam, North Fork American at North Fork Dam, Merced at Pohono Bridge, and Kings at Pine Flat).

Each basin was calibrated and verified by the California-Nevada River Forecast Center (NOAA CNRFC) using parts of the 6-hour and daily 1950 to 1993 precipitation, temperature, and streamflow time series. A 30-year climatological verification for the 1963-1992 period using the CNRFC calibration parameters was performed in this study, as it is the most complete and is close to the NCDC 1961 to 1990 climatology. Comparison of the observed to simulated climatological streamflow for 1963-1992 resulted in monthly streamflow correlation coefficients greater than 0.95 for each of the six basins.

Incremental Perturbations

Streamflow was forced by imposing six incremental sets of constant temperature shifts ($T_{shift,incr}$) and precipitation ratios ($P_{ratio,incr}$) on the historical MAT and MAP time series (Table 2). The selected incremental values represent the upper and lower bounds of the mid- and late 21st century GCM projected changes. Adjusted 6-hour temperature and precipitation input data were calculated by uniformly adding the temperature shift, and multiplying by the precipitation ratio, for each temperature and precipitation time series ($T_{incr}(t) = T(t)_{hist} + T_{shift,incr}$; $P_{incr}(t) = P(t)_{hist} * P_{ratio,incr}$). For each of the six incremental changes, daily streamflow ($Q_{day,incr}$) was simulated at each of the representative basins. From these daily streamflow outputs, monthly mean-daily streamflow, in cubic meters per second daily (CMSD), was computed for the time period October 1963 to September 1992. Monthly climatological means were computed as the monthly mean-daily streamflow for each calendar month over the 30 year period ($Q_{month,incr}$). Monthly means were also calculated for each observed 1963 to 1992 streamflow time series to provide historical mean-monthly baseline climatologies ($Q_{month,hist}$).

Temperatue Shift ^{o}C	Precipitation Rato
1.5	1.00
1.5	1.09
3.0	1.00
3.0	1.18
5.0	1.00
5.0	1.30

Table 2. The six specified incremental temperature shifts and precipitation ratios.

Scenario Perturbations

A warm wet GCM climate projection based on the Hadley Centre's HadCM2 run 1 and a cool dry climate projection based on the NCAR PCM run B06.06, relative to the mean of the IPCC GCM projections were selected as end member-climate scenarios. From these coupled atmosphere-ocean GCM simulations, two 30 year periods (2010 to 2039, 2050 to 2079), and one 20 year period (2080 to 2099) were used. The GCM data were statistically downscaled and interpolated to a mean-monthly temporal and 10 km spatial resolution using historically derived regression equations based on the PRISM technique (Daley et al. 1999). Monthly temperature shifts and precipitation ratios derived from the mean-area basin climatologies were then imposed on the historical 1963 to 1992 temperature and precipitation time series as in the incremental studies. The California 10 km resolution temperature shifts (Fig. 2) averaged for each climatological period indicates that statewide, the PCM temperature difference increases to about 1.5 ^{o}C by 2050 and to 2.4 ^{o}C by 2100, while the HadCM increases to about 2.4 ^{o}C by 2050 and to 3.3 ^{o}C by 2100. The precipitation ratios (Fig. 3) indicate that PCM precipitation is reduced to about 0.91 of present precipitation by 2010-2039, 0.86 by 2050-2079 and 0.76 by 2080-2099, while the HadCM2 precipitation ratio increased to about 1.22 by 2010-2039, 1.32 by 2050-

2079, and 1.62 by 2080-2099. This coarse climatology indicates the overall spatial variations, but not the seasonal variations of the changes.

GCM-based monthly mean-area precipitation and temperature were determined for each upper and lower subbasin as the mean of the 10 km gridded temperature and precipitation within the subbasin. Similarly, a set of basin mean-area historical monthly MAP and MAT time series were derived from the available 10 km derived historical data for 1963-1992. Baseline climatological monthly MAP and MAT values were calculated from these 30 year records.

A ratio (shift) between the monthly basin mean area MAP_{scen} (MAT_{scen}) climatologies for the projection time periods and the monthly baseline historical precipitation (temperature) climatologies were computed. These climate scenario precipitation ratios ($P_{ratio,scen}$) and temperature shifts ($T_{shift,scen}$) were used to adjust the archived NWS observed time series in a similar manner as the constant incremental values, but in this case with monthly adjustments. The imposed climate scenario mean-area precipitation and temperature time series were used as input to the hydrologic models as described in the incremental approach.

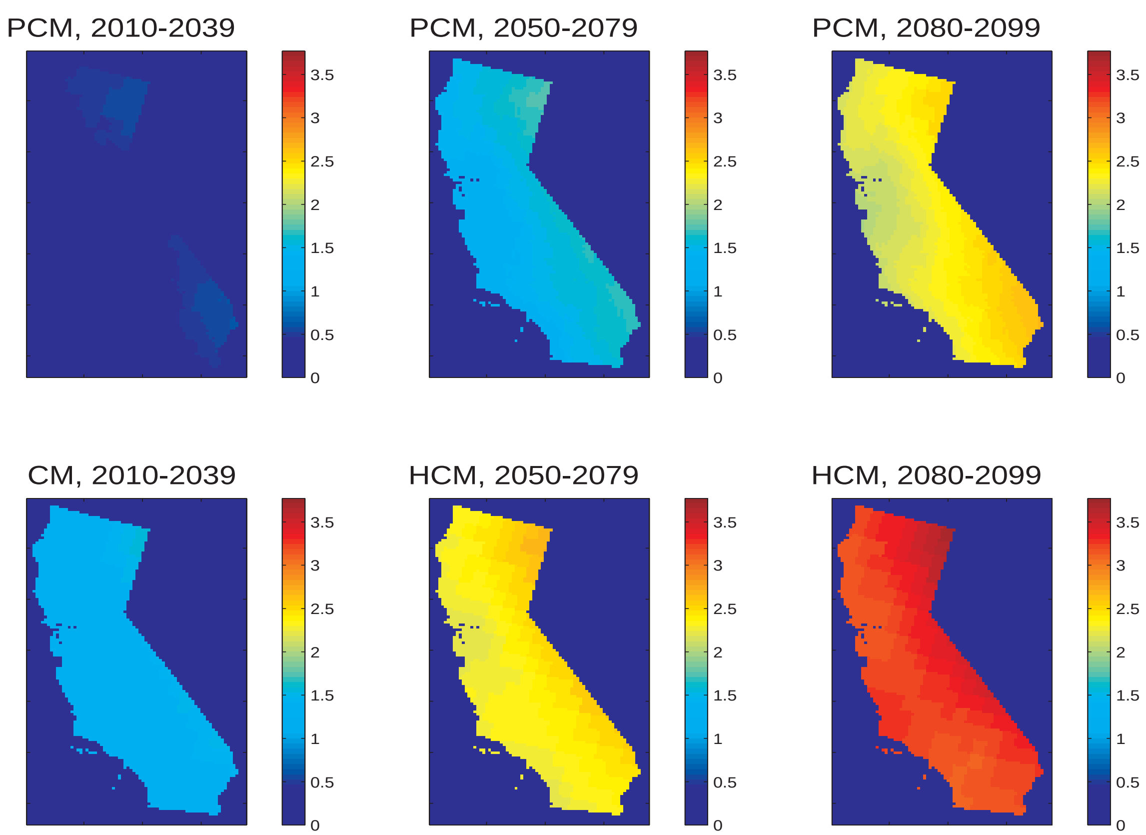

Figure 2. California climatological temperature shifts (°C) for PCM and HadCM2 averaged over the time periods 2010-2039, 2050-2079, and 2080-2099.

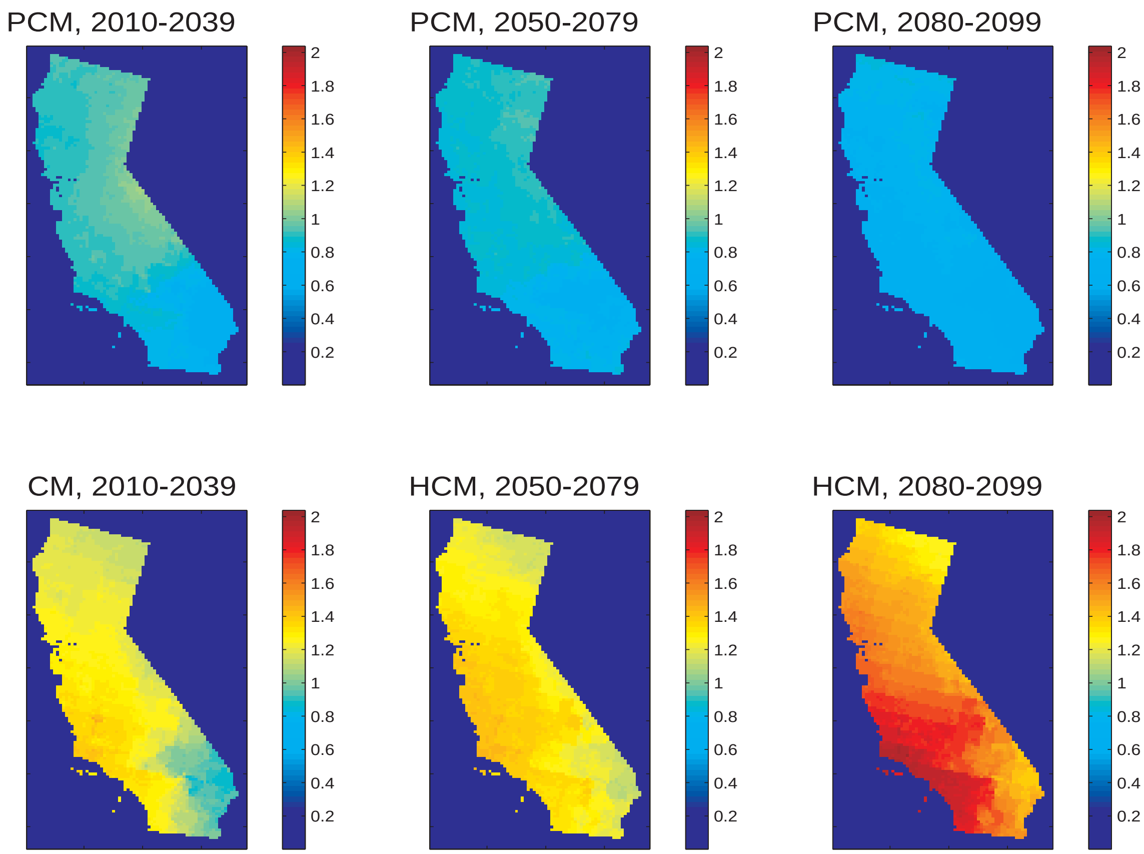

Figure 3. California mean-area climatological precitation ratios for PCM and HadCM2 averaged over the time periods 2010-2039, 2050-2079, and 2080-2099.

RESULTS

Analysis of temperature, precipitation, snow-to-rain with elevation, snowmelt, and streamflow are based on the mean monthly climatologies. Shifts in the cumulative streamflow and exceedance probabilities of peak streamflow were based on the daily 30 year time series and annual peakflow.

Temperature

Figure 4 shows the annual temperature cycle at three of the headwater study basins (Sacramento, American, Merced) for the two GCM projections (HadCM2 and PCM) superimposed on the NWS observed data. The simulated temperature climatologies generally follow the historical seasonal trends, with quasi-linear increases with time. The greatest increases from the baseline are during the JJA season, and in January, with the largest increase during HadCM2 2080-2099, followed by HadCM2 2050-2079, then PCM 2080-2099. The monthly temperature shift ranges are 0.53 ^{o}C to 4.70 ^{o}C for the HadCM2 and –0.14 ^{o}C to 3.00 ^{o}C for the PCM (Tables A1).
The sensitivity of snowmelt to the temperature increases depends on how many degrees the baseline (verification) temperature is below freezing during these months. The high

elevation upper Merced and Kings, where the DJF temperatures are several degrees below freezing is less sensitive to small temperature increases than the upper American, where the DJF temperatures are about one degree C below freezing. The increased summertime heating will increase evapotranspiration, and therefore reduce soil moisture storage and streamflow.

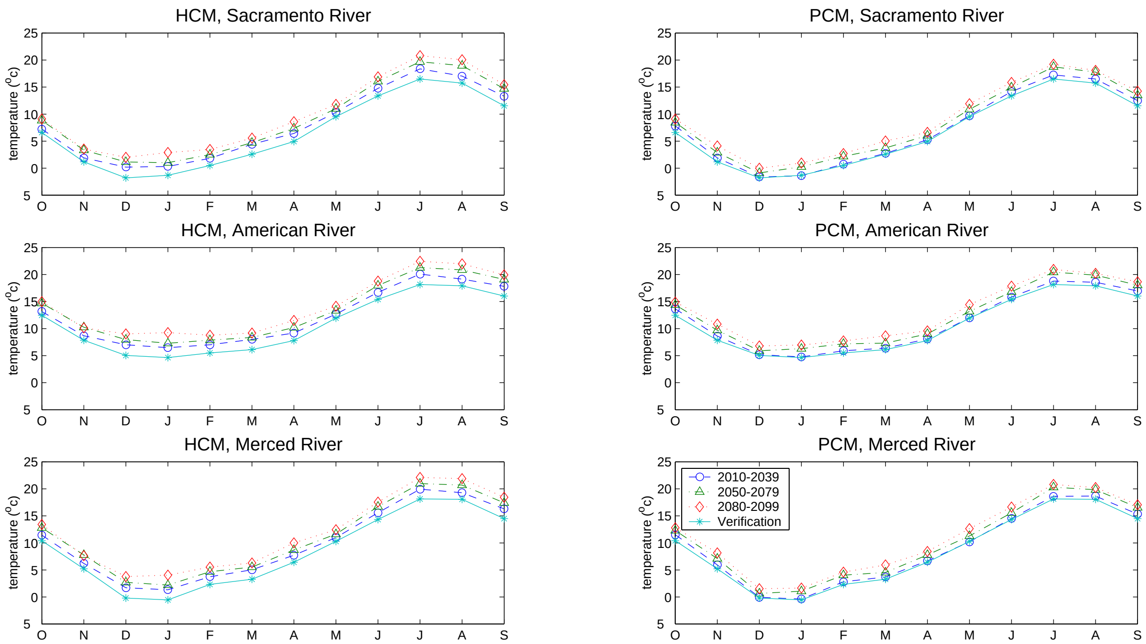

Fig. 4. HadCM2 (HCM) and PCM temperature shifts imposed on the NWS observed temperatures at the Sacramento, American, and Merced study basins.

Precipitation

The mean-monthly precipitation for the same three headwater basins discussed above is shown in Fig. 5. The simulated future climate mean-monthly precipitation volumes do not follow the historical cycle closely. The warm, wet HadCM2 increases in monthly amounts during November to March, and generally shifts the maximum precipitation by about one month later in the year. The PCM total annual precipitation is close to the historical precipitation, however there is decreased precipitation during November to December and again during March and April for the 2050-2079 and 2080-2099 mean climates. In January, the 2050-2079 period shows a large increase, whereas the other months show a significant decrease.

The wet HadCM2 projection consistently shows higher ratios than the drier PCM projection. The HadCM2 has a minimum wet season precipitation ratio of 0.89 in December 2010-2039 and a maximum of 2.04 times the baseline (verification) during February 2080-2099. The PCM precipitation ratios have a much smaller range, with a wet season minimum of 0.48 times the baseline in November 2080-2099 and a maximum of 1.16 times the baseline in January 2050-2079. The range of PCM precipitation ratios is less than the high incremental precipitation ratio (1.3) and shows a decrease inprecipitation, while the HadCM2 exceeds the high incremental ratio in the Merced and Kings basins for 2050-2079 and in all basins for 2080-2099. The precipitation ratio values are provided in the Appendix (Tables A2).

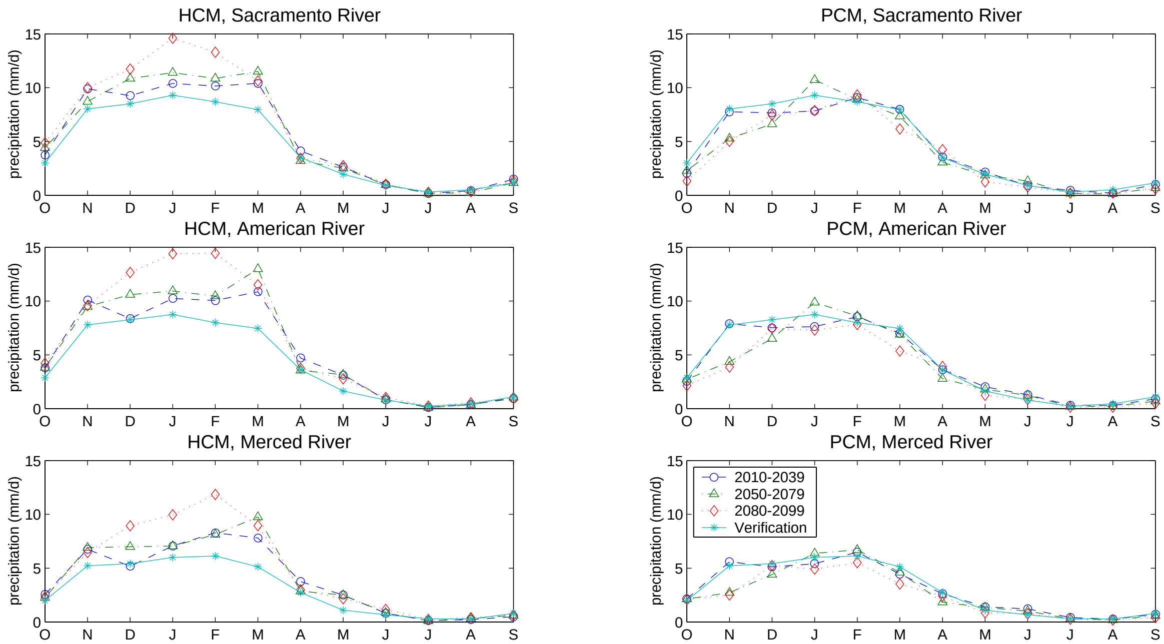

Fig. 5. HadCM2 (HCM) and PCM precipitation ratios imposed on the NWS observed temperatures at the Sacramento, American, and Merced study basins.

Snow-to-Rain

The snow-to-rain ratios vary significantly with latitude and most importantly the level of the lower and upper basins. In this study, the elevation band partition was based on the historical snow accumulation line. The Anderson Snow Model's area elevation curve and the snow-to-rain line determines the percentage of the subbasin's area which is snow covered and determines how that snow covered area changes over time. This removes the need for a large number of elevation band subbasins for determining the percent snow and percent rain within each subbasin area.

The lower subbasins typically have minimal to no accumulation and the upper subbasins have the majority of the accumulated snow. High elevation subbasins (e.g. Upper Merced at 2591 m) result in higher snow accumulation and later season runoff than the lower elevation subbasins (e.g. Upper Sacramento at 1798 m) for the climate change scenarios. The elevation dependent snow-to-rain ratios shift in amount for each projection (Fig. 6). Although the HADCM2 projections show a significant increase in total precipitation, and the PCM projections show reduced precipitation, both cases show a significant reduction of the snow-to-rain ratio.

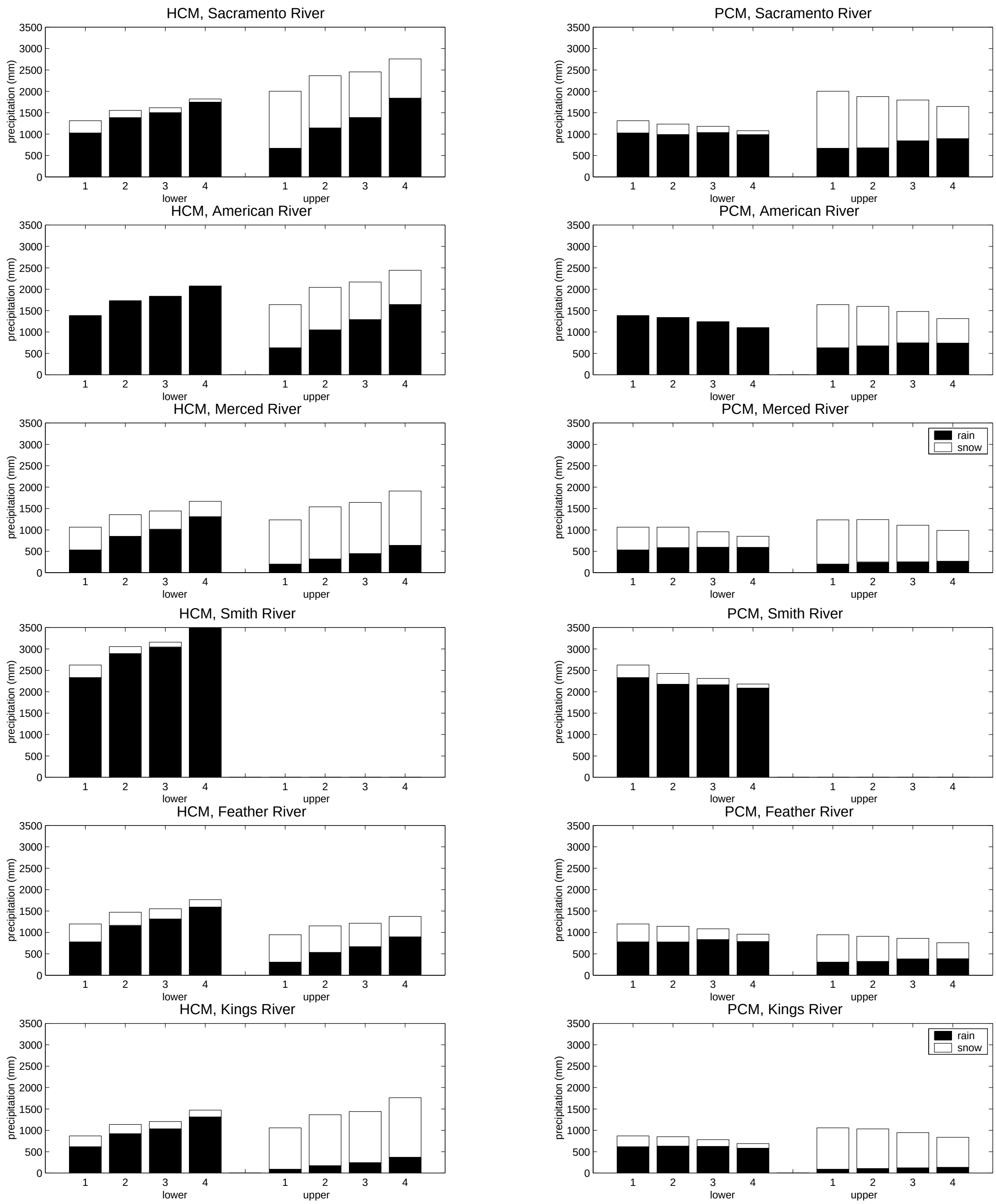

Fig. 6 Snow (clear) and rain (solid) mean annual depth for the lower and upper subbasins for each climate (1) baseline, (2) 2010-2025, (3) 2050-2079, and (4) 2080-2099.

Snow Water Equivalent

Fig. 7 shows the change relative to the baseline snow water equivalent for the snow producing upper and lower subbasins. The Snow Water Equivalent (SWE) decreases for most basins, except the very high Kings Basin (73% of the basin area is in the upper subbasin which has a center of elevation at 2743 m) using the wet and warm HadCM2. The peak snowmelt month similarly shifts earlier for the low elevation basins and is unchanged for the high ones. For the PCM projections, the snow water equivalent is significantly reduced, and the peak is earlier for all basins by 2080-2099. The critical factor is whether the historical temperature is sufficiently below freezing for the snowpack to be unaffected by a small temperature increase.

In all cases (except the very high elevation Kings), the SWE decreases as temperature increases. In general, higher elevation basins are less sensitive and do not lose as much winter season snow pack as those with centroid elevations near the freezing line. The proportion of time (6-hr timesteps) the upper subbasins are below freezing during January is given in Table 3. The HadCM2 proportion of January that is below freezing decreases by more than 50%, while the PCM decreases by about 25%. The large difference is due to the differences in the rate of projected warming.

	Sacramento	Feather	American	Merced	Kings
Baseline	0.7140	0.6710	0.5634	0.6621	0.7002
H 2025	0.5538	0.5215	0.4368	0.5336	0.5619
P 2025	0.7228	0.6661	0.5556	0.6532	0.6895
H 2065	0.4941	0.4591	0.3782	0.4645	0.5014
P 2065	0.5624	0.5336	0.4470	0.5554	0.5901
H 2090	0.3153	0.3164	0.2478	0.3134	0.3546
P 2090	0.5005	0.4731	0.3989	0.5129	0.5449

Table 3. Proportion of January 6-hour timesteps below freezing for each upper basin where H represent HadCM2 and P represents PCM for projected climatological periods 2025 (2010-2029), 2065 (2050-2079), and 2090 (2080-2099).

Snowmelt

Snowmelt and rain represent the liquid water input for evaporation, infiltration, and streamflow response. The increased temperature and precipitation for the HadCM2 simulation yields a consistent early season increase in the liquid water input to the hydrologic system as the projections go from 2010 to 2099. Likewise, the relatively cool and dry PCM projection, with temperatures increasing at a slower rate, results in earlier season snowmelt. The peak timing for each simulation shifts towards earlier in the year as the snow-to-rain ratio decreases. The change in the liquid water amount is more pronounced in the lower elevation basins during the early part of the century and then shifts to the higher elevation basins towards the end of the century. This is due to the proximity of the freezing line to the lower basins. As the freezing line moves to higher elevation, the percent area that is melting in the lower basin is increased.

An evaluation of the ratio of monthly climate change to baseline snowmelt (Fig. 8) shows a large increase for the American, Merced, and Kings during DJF and a large decrease during MJJ for the HadCM2. A similar, but smaller shift occurs for the cooler and drier PCM.

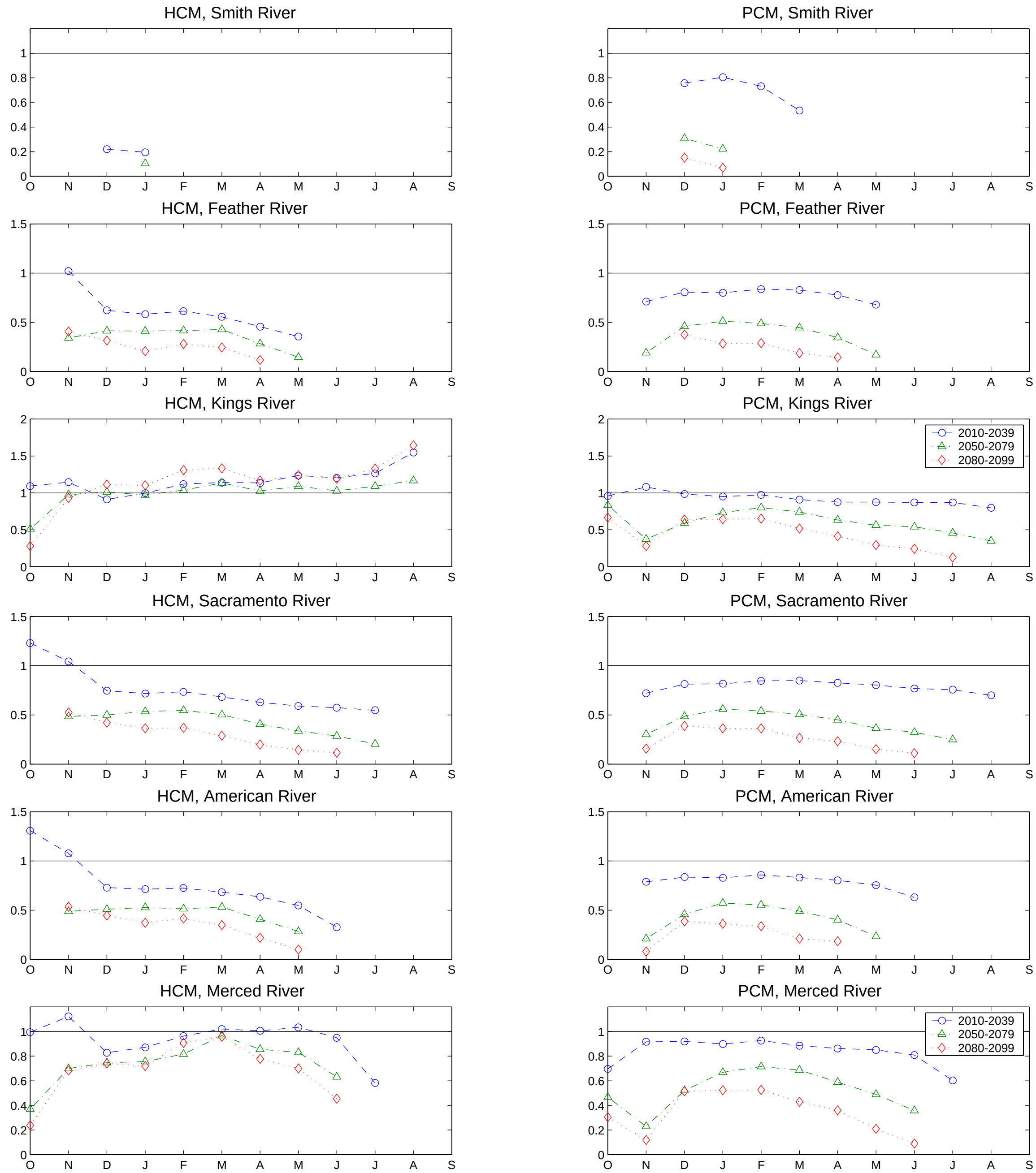

Fig 7. Ratio of climate change to baseline mean-monthly Snow Water Equivalent (SWE) for each basin.

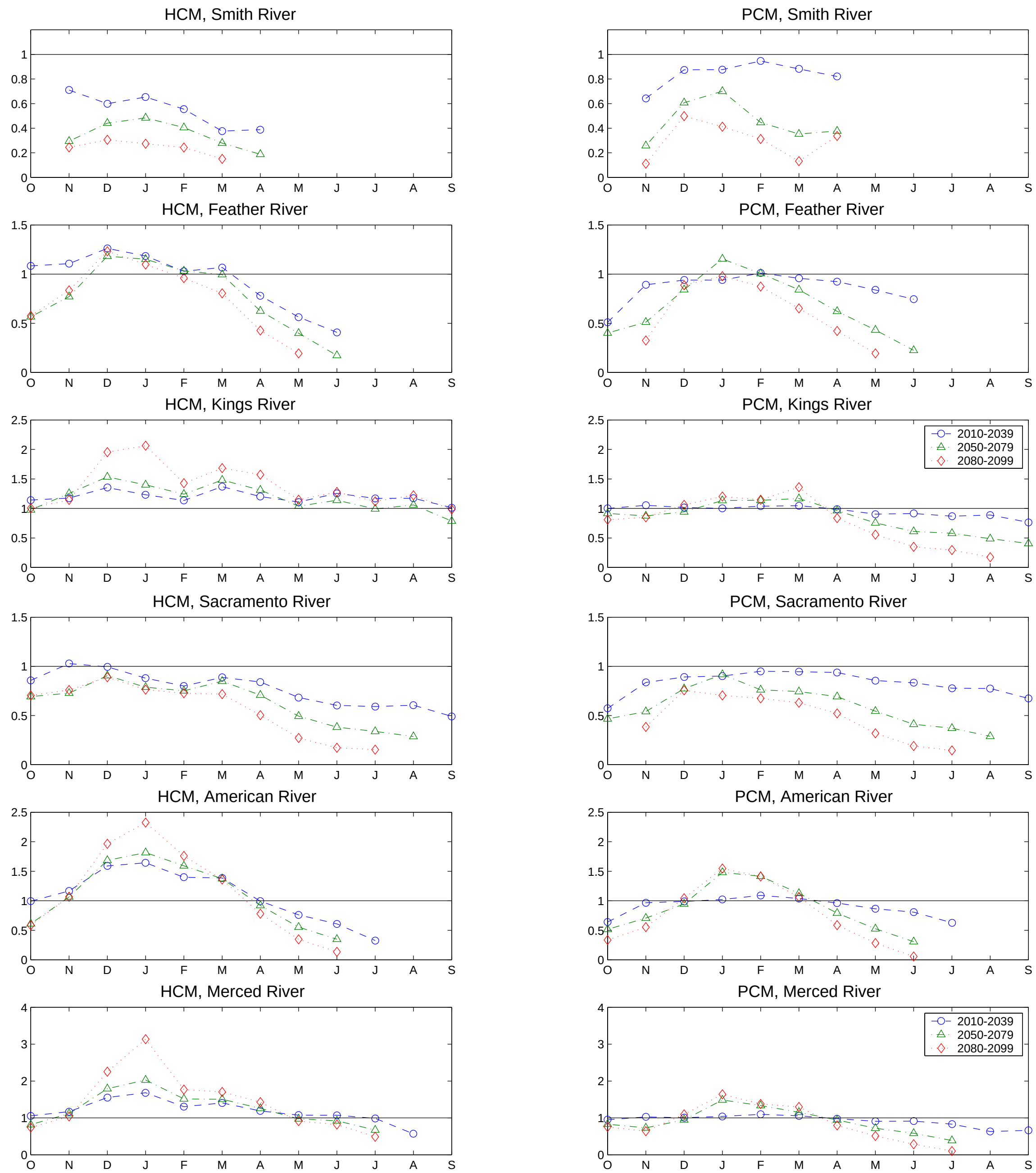

Fig. 8. Ratio of climate change to baseline mean-monthly snowmelt for each basin.

Streamflow

The nonlinear streamflow response as forced by temperature and precipitation change is sensitive to the characteristics of the basin, particularly the snowline elevation and local weather pattern. Fig. 9 shows the mean-monthly climatological streamflow for the study basins forced by the two GCM-simulated temperature shifts and precipitation ratios imposed on the historical time series. The warm and wet HadCM2-forced streamflow shows large increases in total annual streamflow, increases during the DJF and MAM seasons (for most of the basins), and earlier peakflow timing for the 2080-2099 period. The cool and dry PCM-forced streamflow shows a modest increase in DJF flow volume and decreased JJA streamflow.

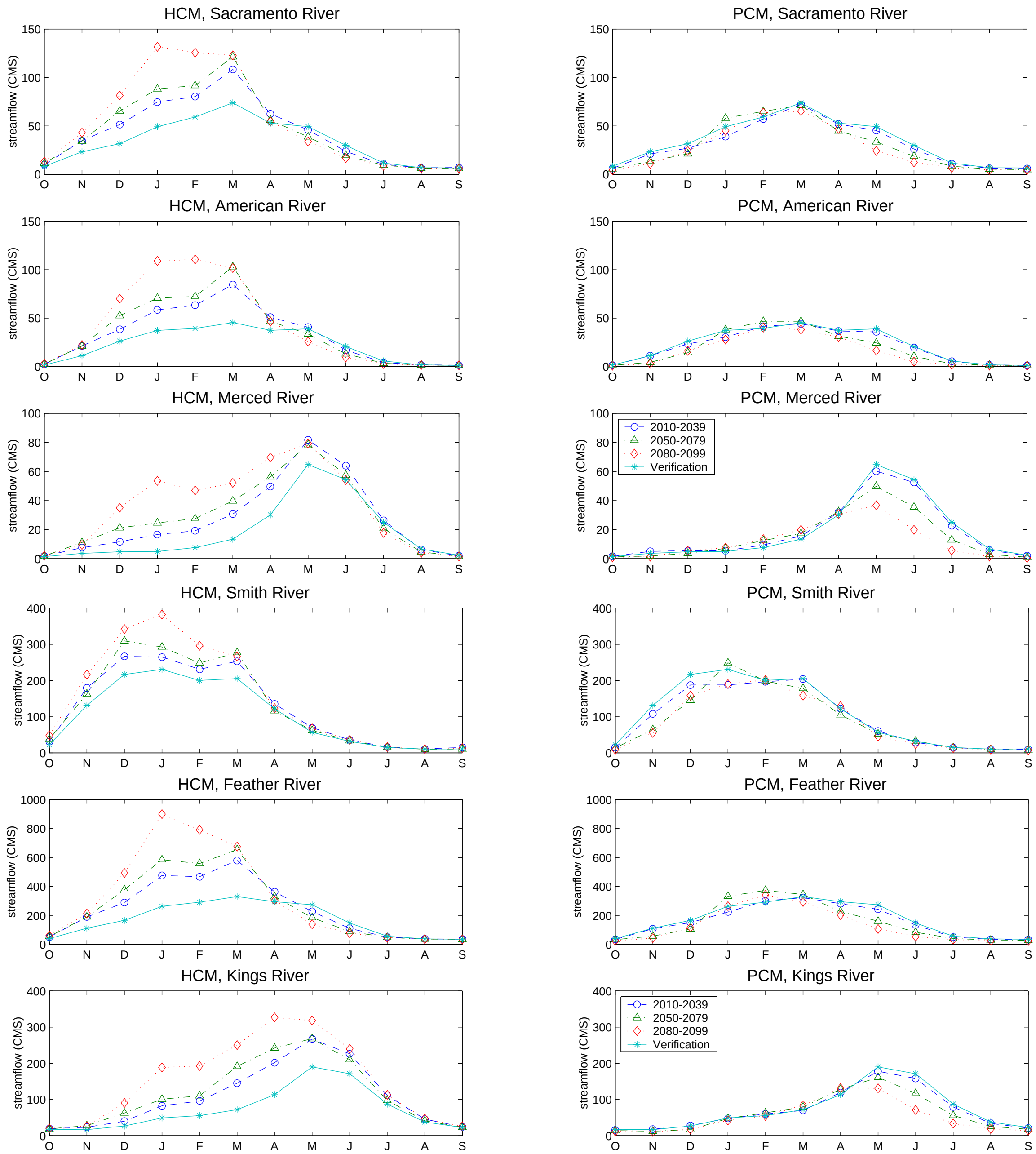

Fig. 9. Streamflow monthly climatologies based on the HadCM2 (HCM) and the PCM.

The runoff coefficient (streamflow divided by precipitation) increases during NDJFM and decreases during AMJJ for the upper subbasins as forced by both GCM scenarios.

This is consistent with the increasing number of days above freezing for each subbasin.

The incrementally uniform shifts in streamflow response are shown in Fig. 10. The low end climate change is represented by 1.5 ºC increase with 0% and 9% precipitation increase. The upper end uniform increase is represented by 5 ºC with 0% and 30% precipitation increase. For the basins studied, a 1.5 ºC increase is not sufficient for an earlier monthly peakflow. This does, however, show up at 3 ºC for the Kings, and 5 ºC for the other snow accumulating subbasins. For all of the snow accumulating basins evaluated, the DJFM monthly streamflow volume increases above the baseline and the MJJA decreases below the baseline.

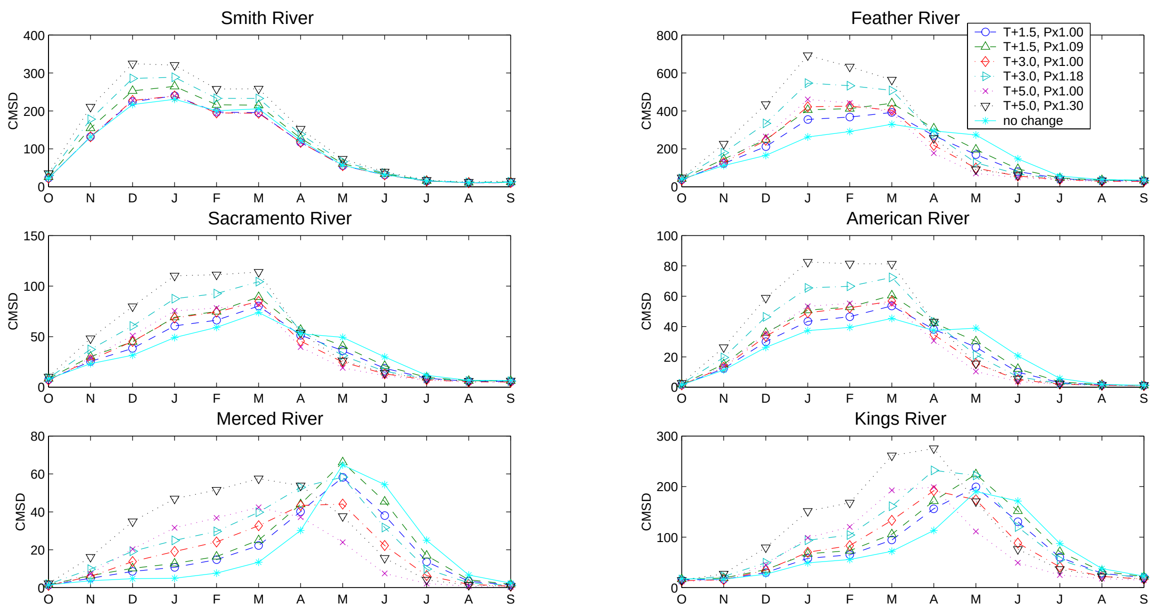

Fig. 10. Streamflow monthly climatologies based on the specified incremental changes.

Cumulative Streamflow

The cumulative daily streamflow, starting from the beginning of each water year (October 1) is plotted in Fig. 11. For both simulations, the day in which 50 percent of the annual flow has occurred is earlier, as the projected streamflow goes from 2010 to 2100. The HadCM2 is very pronounced with large shifts in both the amount and timing, while the PCM shows mainly a shift in timing and reduced magnitude. This is consistent with the PCM precipitation ratio decreasing. The HadCM2 streamflow shifts between 30 and 60 days earlier and the PCM is less than or about 30 days near 2100.

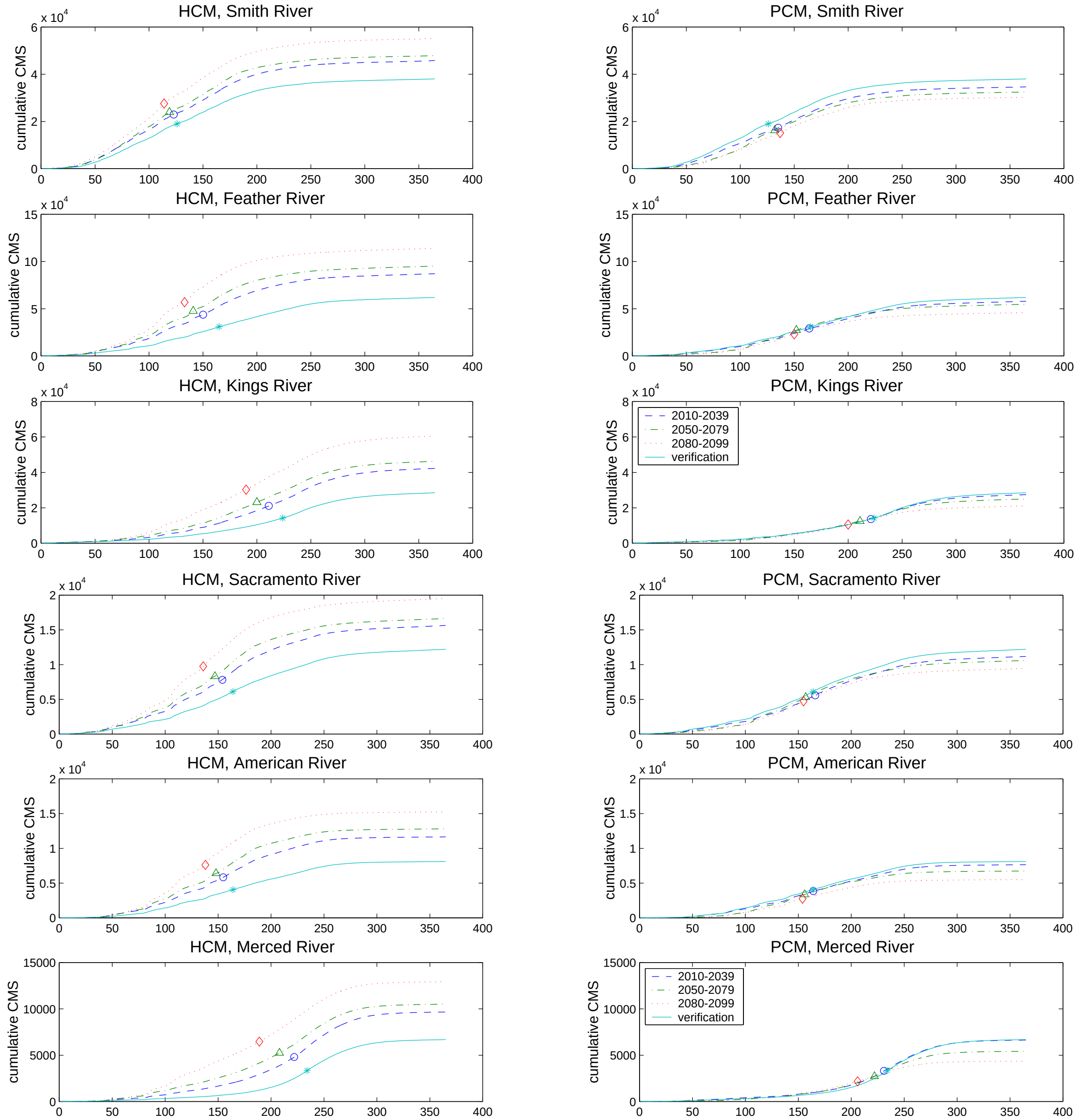

Fig. 11. The cumulative daily streamflow for each basin, where day 1 is October 1 and the mode is marked with a symbol.

Exceedance Probabilities

Changes in the SWE coupled with increased winter time warm precipitation (rain) suggest the increased likelihood of more extreme events, such as floods. Ranking each set of 30 year peak annual daily flows and generating probability of exceedance plots (Fig. 12) indicates that for both the warm and wet HadCM2 and the cool and dry PCM there is a significant increase in the likelihood of high flow days. For each curve shown, the mean annual maximum daily flow is at the 50% exceedance interval. Inspection of this figure points to the very large increase in high flow occurrence, and a 5% exceedance high flow for the projected climates that far exceeds current conditions.

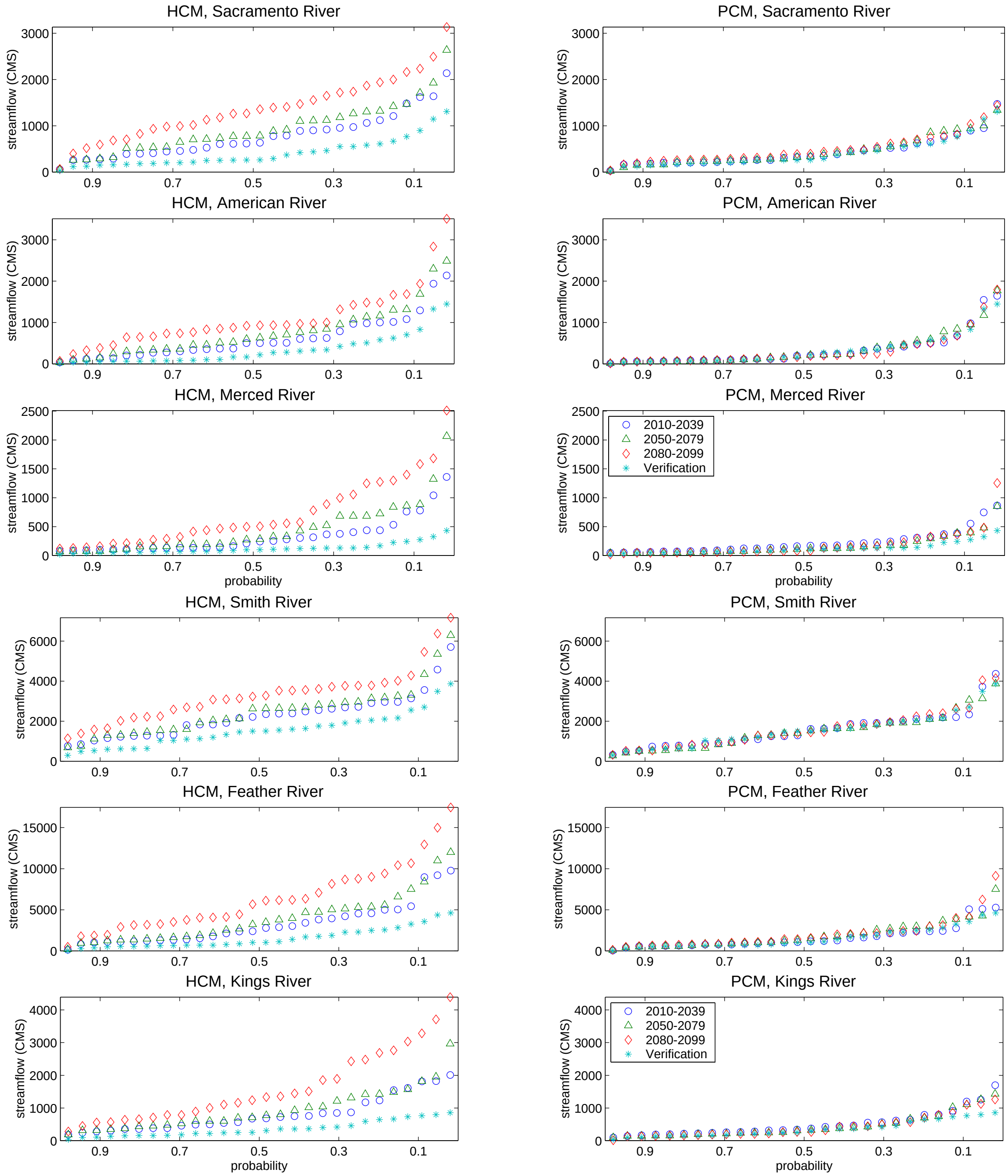

Fig. 12. Exceedance probabilities of the peak daily flow for each year for each climate change scenario.

SUMMARY

An analysis of California hydrologic response due to temperature shifts and precipitation ratios based on two GCM-projections and six specified uniform changes was performed. Streamflow and snowmelt timing shifts are discussed as lower and upper bounds of the set of possible outcomes. For all cases, there are fewer freezing days with climate change than present day during the snowpack storage months. More water flows through the system in the winter and less will be available during the dry season. An important result that appears for all cases considered, is the large shift in the likelihood of high flow days.

The above results suggest that the range of possible climate change responses are due to large-scale change and local characteristics. This could be intensified if there are large-scale frequency and/or intensity changes in natural low frequency variations (e.g. ENSO, PDO, AO). Large-scale weather patterns that influence precipitation and runoff timing may dynamically shift, with significantly different local climates.

In this study, monthly changes were superimposed on the historical dataset, therefore the effects of more intense rainfall events were not represented. The predicted decreasing diurnal temperature ranges (IPCC TAR 2001) were also not represented by this method.

CONCLUSION

Determining the impacts of climate change on water resources by evaluating the response of the SAC-SMA to end-member scenarios and incremental changes is a valid approach. By using these operational models for simulating and analyzing hydrologic response to climate change, increased credibility and public acceptance is likely. The temperature shifts and precipitation ratios imposed on the historical time series constrain the results to perturbations about the historical. This approach removes the variance in the climate change time series that indicate extreme events. However, this is the current impact assessment approach and this study will be useful for applications of water demand and agro-ecomomic assessments.

Interpreting the results should remain somewhat qualitative due to the overall uncertainty in model projections. The weak assumption of fixed land use results in surface characteristics in both the GCMs and the SAC-SMA that do not adequately represent future energy and water budgets. Using the SAC-SMA with a fixed ET demand curve can not explicitly yield ET climate change response with temperature, which is important during the dry down MAMJJA period. This implies that the simulated streamflow is higher than it should be during these periods of evapotranspiration depletion. This effect is not significant during the snow accumulation period and is of less magnitude than GCM uncertainties, such as cloud fraction.

There are a number of aspects of future climate simulation analysis studies that need to be extended. First, there is a need to further evaluate the GCM results and reduce the model bias. There is a need for more GCM ensemble members of the most recent simulations. Archived sub-daily time series will reduce the amount of statistical interpolation and again reduce some errors. Second, dynamic downscaling needs to be incorporated into these studies. A key question is, what scale is of most importance in capturing orographically produced precipitation in California? Certainly GCM resolutions are not sufficient, even with the statistical downscaling applied. Another important question is; How many downscaled runs are required and should there be an ensemble of downscaled simulations for each GCM simulation? Third, there is a need to improve ET as a temperature dependent derivation and channel routing for capturing the timing more accurately in the SAC-SMA.

Given the above deficiencies, this study does provide an important and reasonable set of upper and lower bounds of hydrologic response to climate change in California. Climate models will never predict the future, but can provide projections with an uncertainty that can be bracketed. It is these bracketed solution sets that may ultimately provide water resources decision-makers with the type of information needed to safeguard one of our more important natural resources.

Acknowledgements: We thank the NOAA/NWS California Nevada River Forecast Center for their collaboration with us on the application of the SAC-SMA and providing historical streamflow data. We thank the National Center for Atmospheric Research and the Hadley Centre for providing the AOGCM output. We also thank Ron Nielson and Chris Daley of Oregon State University for providing statistically interpolated 10 km resolution historical and projected precipitation and temperature time series. Sue Kemball-Cook's help mapping the 10 km fields onto the target watersheds is much appreciated. This project is part of a California Energy Commission (CEC) study on the impacts of climate change in California. This project was supported by the Stratus Consulting Company via funds provided to EPRI by the CEC. Work at the Department of Energy is under contract DE-AC03-76F00098.

REFERENCES

Anderson, E.A., 1973: National Weather Service River Forecast System: Snow Accumulation and Ablation Model. NOAA Tech. Memorandum NWS HYDRO-17.

Burnash, R.J.C., R.L. Ferral, and R.A. McQuire, 1973: A generalized streamflow simulation system. In Conceptual Modeling for Digital Computers. U.S. National Weather Service.

Daly, C., T.G.F. Kittel, A. McNab, J.A. Royle, W.P. Gibson, T. Parzybok, N. Rosenbloom, G.H. Taylor, and H. Fisher. 1999: Development of a 102-year high resolution climate data set for the conterminous United States. In: Proceedings, 10th Symposium on Global Change Studies, 79th Annual Meeting of the American Meteorological Society, 10-15 January, Dallas, TX, 480-483.

Gleick, P.H., 1987: The development and testing of a water balance model for climate impact assessment: Modeling the Sacramento basin. Water Resources Research, 23, 1049-1061.

Jeton, A.E., M.D. Dettinger, and J.L.. Smith, 1996: Potential effects of climate change on streamflow: Eastern and western slopes of the Sierra Nevada, California and Nevada.

U.S. Geological Survey, Water Resources Investigations Rep. 95-4260, 44pp.
Knowles, N. and D.R. Cayan, 2001: Global climate change: Potential effects on the Sacramento-San Joaquin watershed and the San Francisco Estuary. http://meteora.ucsd.edu/~knowles/papers/Globaland California.pdf
Leavesley, G.H., R.W. Litchy, M.M. Troutman, and L.G. Saindon, 1983: Precipitation-Runoff Modeling System UserÕs Manual. U.S. Geological Survey Water Resources Investigations Report 83-4238. 207 pp.
Lettenmaier, D.P. and T.Y. Gan, 1990: Hydrologic sensitivities of the Sacramento-San Joaquin River Basin, California, to global warming. Water Resources Research, 26, 69-86.
Miller, N.L., J. Kim, R.K. Hartman, and J. Farrara, 1999: Downscaled climate and streamflow study of the Southwestern United States. J. American Water Resources Association, 35, 1525-1537.
Revelle, R.R. and P.E. Waggoner,1983: Effects of a carbon dioxide induced climatic change on water supplies in the Western United States. In Changing Climate, National Academy of Sciences Press, Washington, D.C.
Thornthwaite, C.W. and J.R. Mather, 1948: The water balance. In Publications in climatology, Laboratory of Climatology, Drexel Inst. Technology, Centerton, N.J. 81, 104 pp.
Wigley, T.M.L. and S.C.B. Raper, 2001: Interpretation of high projections for global-mean warming. Science, 293, 451-454.
Wilby, R.L. and M.D. Dettinger, 2000: Streamflow changes in the Sierra Nevada, California, simulated using statistically downscaled general circulation model output. In Linking Climate Change to Land Surface Change, Ed. S. McLaren and D. Kniven, Kluwer Academic Pub., 99-121.

APPENDIX: Tables for the CEC Impacts Studies

APPENDIX A1: Temperature Shifts ^oC

The gray rows represent the upper subbasins and the clear rows are the lower subbasins.

	Smith	Sacramento	Feather	American	Merced	Kings
Jan		1.642	1.852	1.847	1.920	1.989
	1.495	1.637	1.783	1.809	1.872	1.918
Feb		1.339	1.524	1.528	1.411	1.301
	1.299	1.337	1.459	1.500	1.415	1.310
Mar		1.852	1.990	1.892	1.787	1.714
	1.653	1.840	1.913	1.856	1.741	1.650
Apr		1.498	1.477	1.396	1.284	1.197
	1.384	1.492	1.461	1.397	1.288	1.206
May		0.791	0.697	0.735	0.651	0.523
	0.963	0.796	0.722	0.753	0.705	0.607
Jun		1.403	1.359	1.304	1.281	1.347
	1.357	1.391	1.313	1.285	1.263	1.310
Jul		1.870	2.028	1.947	1.849	1.867
	1.626	1.861	1.976	1.919	1.801	1.794
Aug		1.294	1.245	1.224	1.213	1.184
	1.308	1.288	1.218	1.213	1.206	1.176
Sep		1.775	1.868	1.806	1.861	2.006
	1.581	1.763	1.808	1.776	1.814	1.941
Oct		0.631	0.531	0.702	1.000	1.077
	0.988	0.649	0.577	0.722	1.040	1.143
Nov		0.739	0.724	0.820	0.962	1.002
	0.925	0.747	0.716	0.820	0.997	1.060
Dec		1.986	2.045	1.986	1.940	2.007
	1.865	1.978	1.993	1.962	1.910	1.952

A1a. Temperature shifts HADCM2 2010-2039

	Smith	Sacramento	Feather	American	Merced	Kings
Jan		2.323	2.607	2.666	2.779	2.808
	2.248	2.322	2.523	2.623	2.750	2.768
Feb		2.023	2.339	2.387	2.368	2.276
	1.982	2.021	2.231	2.336	2.353	2.259
Mar		2.136	2.246	2.242	2.253	2.170
	2.111	2.135	2.202	2.223	2.246	2.169
Apr		2.423	2.517	2.403	2.290	2.272
	2.176	2.413	2.475	2.389	2.267	2.240
May		1.459	1.325	1.380	1.281	1.057
	1.639	1.465	1.373	1.411	1.351	1.163
Jun		2.688	2.731	2.591	2.433	2.517
	2.457	2.675	2.690	2.569	2.380	2.419
Jul		3.196	3.333	3.152	2.921	2.955
	2.778	3.177	3.264	3.116	2.846	2.830
Aug		3.240	3.181	2.951	2.688	2.717
	2.911	3.216	3.114	2.921	2.623	2.617
Sep		3.177	3.218	3.080	2.975	3.103
	2.874	3.164	3.190	3.063	2.918	3.020
Oct		2.230	2.187	2.235	2.389	2.530
	2.373	2.237	2.201	2.240	2.394	2.541
Nov		2.160	2.337	2.415	2.561	2.627
	2.157	2.166	2.314	2.404	2.566	2.638
Dec		2.950	2.988	2.947	2.917	2.898
	2.847	2.940	2.931	2.922	2.898	2.868

A1b. Temperature shifts HADCM2 2050-2079

	Smith	Sacramento	Feather	American	Merced	Kings
Jan		4.235	4.701	4.647	4.661	4.675
	3.841	4.216	4.523	4.558	4.569	4.543
Feb		2.964	3.266	3.294	3.221	3.054
	2.900	2.960	3.159	3.247	3.218	3.065
Mar		2.987	3.106	3.066	3.001	2.794
	2.904	2.978	3.026	3.034	2.992	2.797
Apr		3.667	3.858	3.730	3.611	3.489
	3.261	3.650	3.785	3.700	3.570	3.445
May		2.257	2.095	2.172	2.084	1.850
	2.472	2.265	2.160	2.212	2.173	1.986
Jun		3.528	3.542	3.409	3.281	3.318
	3.294	3.508	3.475	3.378	3.233	3.227
Jul		4.325	4.530	4.325	4.057	4.116
	3.862	4.310	4.471	4.293	3.973	3.982
Aug		4.330	4.285	4.075	3.897	3.996
	4.090	4.309	4.212	4.037	3.812	3.871
Sep		3.915	4.005	3.937	4.024	4.293
	3.759	3.909	3.960	3.907	3.955	4.199
Oct		2.497	2.362	2.534	2.970	3.167
	2.870	2.505	2.369	2.535	2.994	3.212
Nov		2.369	2.178	2.272	2.357	2.283
	2.666	2.374	2.204	2.297	2.440	2.420
Dec		3.812	4.013	4.005	4.004	3.959
	3.639	3.802	3.928	3.966	3.977	3.925

A1c. Temperature shifts HADCM2 2080-2099

	Smith	Sacramento	Feather	American	Merced	Kings
Jan		-0.078	0.081	0.111	0.163	0.201
	-0.141	-0.075	0.060	0.097	0.160	0.187
Feb		0.250	0.395	0.415	0.486	0.520
	0.146	0.255	0.371	0.392	0.478	0.490
Mar		0.162	0.188	0.264	0.406	0.467
	0.169	0.155	0.216	0.287	0.405	0.466
Apr		0.309	0.325	0.299	0.270	0.345
	0.281	0.310	0.313	0.280	0.260	0.309
May		0.165	0.116	0.058	-0.071	-0.112
	0.171	0.166	0.104	0.047	-0.072	-0.114
Jun		0.811	0.560	0.446	0.204	0.151
	0.844	0.810	0.588	0.458	0.212	0.171
Jul		0.749	0.710	0.654	0.498	0.441
	0.687	0.751	0.713	0.650	0.502	0.450
Aug		0.754	0.727	0.656	0.603	0.659
	0.722	0.756	0.695	0.619	0.590	0.606
Sep		0.954	1.025	0.947	0.869	0.867
	0.842	0.963	0.974	0.896	0.849	0.811
Oct		1.201	1.248	1.209	1.122	1.072
	1.120	1.205	1.224	1.182	1.108	1.037
Nov		0.740	0.753	0.761	0.716	0.655
	0.745	0.739	0.757	0.768	0.719	0.664
Dec		0.156	0.167	0.150	0.145	0.191
	0.172	0.155	0.150	0.128	0.138	0.167

A1d. Temperature shifts PCM 2010-2039

	Smith	Sacramento	Feather	American	Merced	Kings
Jan		1.562	1.710	1.670	1.624	1.633
	1.488	1.568	1.649	1.622	1.615	1.609
Feb		1.691	1.742	1.712	1.727	1.769
	1.654	1.696	1.708	1.681	1.718	1.743
Mar		1.151	1.176	1.196	1.254	1.334
	1.150	1.147	1.188	1.197	1.250	1.324
Apr		1.101	1.196	1.239	1.366	1.498
	1.055	1.101	1.192	1.226	1.353	1.450
May		1.341	1.330	1.240	1.006	0.903
	1.294	1.343	1.304	1.213	1.001	0.890
Jun		1.572	1.501	1.400	1.241	1.286
	1.516	1.576	1.492	1.378	1.235	1.257
Jul		2.242	2.434	2.335	2.192	2.251
	1.952	2.254	2.367	2.257	2.167	2.164
Aug		2.030	2.129	1.996	1.799	1.808
	1.843	2.037	2.057	1.921	1.778	1.738
Sep		1.967	2.078	2.037	2.080	2.128
	1.871	1.972	2.006	1.960	2.043	2.021
Oct		1.855	1.956	1.939	1.905	1.856
	1.757	1.861	1.926	1.912	1.891	1.830
Nov		1.731	1.779	1.835	1.892	1.878
	1.714	1.731	1.799	1.855	1.896	1.889
Dec		0.914	0.886	0.866	0.851	0.883
	0.996	0.913	0.868	0.853	0.851	0.885

A1e. Temperature shifts PCM 2050-2079

	Smith	Sacramento	Feather	American	Merced	Kings
Jan		2.259	2.455	2.350	2.194	2.219
	2.099	2.269	2.362	2.275	2.182	2.184
Feb		2.201	2.251	2.236	2.277	2.308
	2.162	2.206	2.220	2.208	2.269	2.287
Mar		2.442	2.505	2.547	2.652	2.730
	2.354	2.441	2.519	2.554	2.648	2.722
Apr		1.693	1.713	1.782	2.006	2.203
	1.732	1.690	1.718	1.775	1.989	2.138
May		2.384	2.584	2.509	2.384	2.358
	2.160	2.392	2.513	2.432	2.359	2.286
Jun		2.497	2.589	2.474	2.337	2.424
	2.316	2.508	2.530	2.408	2.315	2.348
Jul		2.728	2.920	2.820	2.725	2.862
	2.477	2.738	2.839	2.732	2.694	2.753
Aug		2.351	2.450	2.331	2.198	2.272
	2.181	2.356	2.381	2.257	2.174	2.181
Sep		2.717	2.760	2.660	2.607	2.678
	2.580	2.724	2.695	2.584	2.573	2.567
Oct		2.491	2.513	2.468	2.402	2.400
	2.418	2.493	2.490	2.435	2.385	2.357
Nov		2.935	2.955	2.975	2.938	2.910
	2.877	2.937	2.974	2.998	2.947	2.937
Dec		1.782	1.784	1.768	1.726	1.754
	1.822	1.778	1.776	1.759	1.728	1.764

A1f. Temperature shifts PCM 2080-2099

APPENDIX: A2: Precipitation Ratios

The gray rows represent the upper subbasins and the clear rows are the lower subbasins.

	Smith	Sacramento	Feather	American	Merced	Kings
Jan		1.117	1.165	1.169	1.178	1.255
	1.087	1.121	1.170	1.171	1.181	1.252
Feb		1.166	1.211	1.255	1.341	1.449
	1.177	1.174	1.229	1.263	1.353	1.454
Mar		1.306	1.390	1.454	1.492	1.455
	1.283	1.313	1.413	1.466	1.524	1.492
Apr		1.177	1.264	1.301	1.366	1.382
	1.124	1.181	1.272	1.304	1.373	1.393
May		1.330	1.596	1.898	2.220	2.258
	1.278	1.349	1.665	1.927	2.292	2.335
Jun		1.075	1.107	1.061	1.282	1.350
	1.078	1.079	1.078	1.036	1.214	1.362
Jul		0.545	0.419	0.505	0.408	0.578
	0.738	0.551	0.445	0.602	0.411	0.673
Aug		0.826	0.839	0.837	0.763	0.861
	0.871	0.827	0.845	0.866	0.772	0.903
Sep		1.293	1.010	0.860	0.640	0.665
	1.425	1.288	1.019	0.870	0.608	0.645
Oct		1.248	1.351	1.315	1.281	1.262
	1.187	1.248	1.333	1.327	1.282	1.272
Nov		1.234	1.287	1.296	1.292	1.251
	1.181	1.232	1.277	1.291	1.292	1.253
Dec		1.089	1.044	1.013	0.956	0.954
	1.110	1.087	1.041	1.013	0.954	0.949

A2a. Precipitation ratios HADCM2 2010-2039

	Smith	Sacramento	Feather	American	Merced	Kings
Jan		1.224	1.267	1.249	1.171	1.172
	1.190	1.228	1.270	1.251	1.176	1.175
Feb		1.248	1.285	1.307	1.317	1.358
	1.257	1.253	1.295	1.312	1.326	1.361
Mar		1.444	1.603	1.734	1.857	1.829
	1.407	1.456	1.640	1.753	1.907	1.876
Apr		0.914	0.953	0.984	1.033	1.016
	0.893	0.915	0.955	0.985	1.046	1.034
May		1.279	1.614	1.925	2.246	2.228
	1.171	1.298	1.673	1.938	2.286	2.289
Jun		1.058	1.122	1.107	1.338	1.439
	1.018	1.054	1.083	1.093	1.266	1.449
Jul		0.572	0.392	0.391	0.351	0.613
	0.733	0.572	0.408	0.477	0.346	0.713
Aug		0.483	0.603	0.794	1.086	1.191
	0.533	0.479	0.565	0.778	1.123	1.267
Sep		1.003	1.003	0.956	0.768	0.700
	1.023	1.004	1.012	0.961	0.766	0.710
Oct		1.467	1.456	1.325	1.150	1.089
	1.446	1.465	1.423	1.327	1.134	1.075
Nov		1.084	1.169	1.216	1.314	1.415
	1.067	1.089	1.177	1.219	1.322	1.423
Dec		1.277	1.281	1.282	1.286	1.340
	1.292	1.278	1.281	1.282	1.289	1.334

A2b. Precipitation ratios HADCM2 2050-2079

	Smith	Sacramento	Feather	American	Merced	Kings
Jan		1.568	1.629	1.644	1.657	1.743
	1.551	1.576	1.641	1.648	1.663	1.741
Feb		1.526	1.702	1.801	1.917	2.032
	1.472	1.542	1.735	1.814	1.935	2.039
Mar		1.332	1.448	1.537	1.724	1.902
	1.320	1.347	1.491	1.556	1.747	1.917
Apr		0.986	1.017	1.039	1.084	1.126
	0.987	0.989	1.020	1.040	1.090	1.131
May		1.401	1.579	1.701	1.984	2.239
	1.281	1.412	1.613	1.698	1.971	2.239
Jun		1.109	1.264	1.314	1.736	2.252
	1.085	1.117	1.253	1.307	1.736	2.351
Jul		0.904	0.806	1.005	0.755	0.859
	1.054	0.913	0.870	1.191	0.792	0.914
Aug		0.639	0.887	1.161	1.333	1.434
	0.570	0.642	0.908	1.185	1.389	1.523
Sep		1.165	0.969	0.871	0.850	0.837
	1.291	1.162	0.961	0.873	0.796	0.831
Oct		1.628	1.636	1.465	1.181	1.103
	1.622	1.628	1.602	1.472	1.157	1.077
Nov		1.244	1.226	1.227	1.229	1.318
	1.279	1.248	1.241	1.236	1.236	1.320
Dec		1.377	1.468	1.529	1.641	1.776
	1.364	1.386	1.484	1.535	1.650	1.770

A2c. Precipitation ratios HADCM2 2080-2099

	Smith	Sacramento	Feather	American	Merced	Kings
Jan		0.842	0.869	0.874	0.905	0.930
	0.832	0.844	0.858	0.866	0.901	0.917
Feb		1.045	1.072	1.070	1.060	1.057
	1.023	1.047	1.067	1.065	1.059	1.054
Mar		1.003	0.972	0.942	0.866	0.818
	1.006	1.003	0.970	0.938	0.867	0.824
Apr		1.020	1.010	1.001	0.956	0.909
	1.026	1.020	1.012	1.003	0.958	0.917
May		1.107	1.151	1.232	1.268	1.176
	1.108	1.105	1.176	1.270	1.284	1.217
Jun		0.962	1.601	1.662	1.845	1.798
	0.594	0.994	1.470	1.524	1.812	1.744
Jul		1.469	1.194	1.323	1.361	1.074
	1.275	1.458	1.261	1.403	1.386	1.149
Aug		0.406	0.453	0.647	0.924	0.723
	0.470	0.405	0.456	0.692	0.955	0.772
Sep		0.868	0.777	0.834	0.883	0.825
	0.930	0.864	0.778	0.839	0.886	0.833
Oct		0.678	0.777	0.879	1.078	1.104
	0.701	0.680	0.770	0.888	1.079	1.115
Nov		0.966	0.996	1.014	1.073	1.140
	0.956	0.968	0.993	1.015	1.071	1.136
Dec		0.901	0.908	0.914	0.948	0.945
	0.906	0.902	0.898	0.904	0.943	0.936

A2d. Precipitation ratios PCM 2010-2039

	Smith	Sacramento	Feather	American	Merced	Kings
Jan		1.153	1.160	1.132	1.065	1.050
	1.129	1.155	1.151	1.124	1.065	1.047
Feb		1.022	1.070	1.079	1.094	1.104
	1.001	1.023	1.065	1.072	1.092	1.098
Mar		0.923	0.940	0.928	0.897	0.864
	0.906	0.925	0.929	0.919	0.897	0.867
Apr		0.877	0.824	0.773	0.670	0.640
	0.895	0.876	0.818	0.765	0.670	0.640
May		0.952	1.006	1.092	1.224	1.188
	0.967	0.952	1.014	1.113	1.229	1.208
Jun		1.429	1.600	1.571	1.525	1.595
	1.212	1.436	1.574	1.517	1.509	1.555
Jul		0.579	0.616	0.803	0.995	0.667
	0.481	0.574	0.633	0.871	1.016	0.737
Aug		0.262	0.298	0.462	0.622	0.431
	0.357	0.260	0.337	0.561	0.668	0.506
Sep		0.597	0.573	0.626	0.718	0.707
	0.650	0.597	0.581	0.645	0.721	0.711
Oct		0.761	0.886	0.949	1.068	1.098
	0.713	0.766	0.871	0.951	1.070	1.109
Nov		0.658	0.606	0.564	0.522	0.545
	0.693	0.659	0.596	0.555	0.522	0.541
Dec		0.778	0.778	0.786	0.814	0.805
	0.788	0.779	0.774	0.785	0.814	0.805

A2e. Precipitation ratios PCM 2050-2079

	Smith	Sacramento	Feather	American	Merced	Kings
Jan		0.847	0.854	0.837	0.822	0.845
	0.849	0.848	0.843	0.829	0.820	0.836
Feb		1.073	1.032	0.983	0.901	0.890
	1.092	1.073	1.020	0.972	0.900	0.886
Mar		0.774	0.752	0.722	0.690	0.694
	0.789	0.775	0.738	0.709	0.687	0.684
Apr		1.214	1.164	1.087	0.869	0.742
	1.200	1.214	1.161	1.080	0.875	0.763
May		0.638	0.675	0.753	0.765	0.591
	0.655	0.640	0.694	0.796	0.785	0.650
Jun		0.849	1.058	1.101	1.129	0.937
	0.653	0.862	1.047	1.095	1.133	0.963
Jul		0.654	0.329	0.575	0.850	0.707
	0.706	0.629	0.425	0.684	0.875	0.753
Aug		0.435	0.119	0.292	0.601	0.448
	0.581	0.413	0.162	0.364	0.629	0.500
Sep		0.531	0.437	0.451	0.509	0.495
	0.607	0.529	0.444	0.464	0.510	0.494
Oct		0.444	0.568	0.737	1.037	1.014
	0.469	0.445	0.573	0.766	1.041	1.037
Nov		0.625	0.542	0.500	0.483	0.528
	0.687	0.624	0.531	0.488	0.479	0.512
Dec		0.876	0.890	0.905	0.972	1.003
	0.885	0.877	0.877	0.895	0.967	0.989

A2f. Precipitation ratios PCM 2080-2099

APPENDIX A3: Incrementally-forced Streamflow sensitivity values

	Smith	Sacramento	Feather	American	Merced	Kings
January	1.039	1.234	1.352	1.163	2.160	1.181
February	0.983	1.120	1.262	1.181	1.932	1.168
March	0.951	1.088	1.188	1.181	1.650	1.310
April	0.960	0.973	0.915	1.020	1.329	1.381
May	0.981	0.734	0.622	0.677	0.899	1.047
June	0.988	0.625	0.542	0.483	0.701	0.762
July	0.989	0.759	0.758	0.508	0.548	0.687
August	0.989	0.861	0.862	0.798	0.507	0.751
September	0.992	0.862	0.886	0.912	0.595	0.871
October	0.997	0.903	0.937	0.966	0.864	0.865
November	1.003	1.096	1.095	1.086	1.356	0.983
December	1.034	1.213	1.278	1.144	1.802	1.123

Table A3a. Mean-monthly streamflow ratios for 1.5 ^{o}C T, 0% P

	Smith	Sacramento	Feather	American	Merced	Kings
January	1.148	1.408	1.544	1.360	2.567	1.367
February	1.079	1.265	1.416	1.341	2.145	1.319
March	1.047	1.208	1.336	1.334	1.867	1.469
April	1.050	1.075	1.044	1.134	1.458	1.514
May	1.072	0.827	0.719	0.778	1.022	1.181
June	1.068	0.705	0.636	0.587	0.835	0.886
July	1.037	0.831	0.820	0.605	0.677	0.810
August	1.044	0.935	0.931	0.871	0.628	0.860
September	1.091	0.955	0.958	0.986	0.740	0.955
October	1.147	1.029	1.044	1.155	1.065	0.965
November	1.178	1.299	1.307	1.343	1.749	1.132
December	1.166	1.419	1.503	1.365	2.152	1.339

Table A3b. Mean-monthly streamflow ratios for 1.5 ^{o}C T, 9% P

	Smith	Sacramento	Feather	American	Merced	Kings
January	1.038	1.394	1.605	1.316	3.850	1.428
February	0.971	1.255	1.459	1.328	3.146	1.497
March	0.944	1.149	1.225	1.251	2.435	1.851
April	0.959	0.862	0.742	0.928	1.437	1.693
May	0.980	0.504	0.360	0.401	0.681	0.916
June	0.988	0.442	0.383	0.239	0.409	0.516
July	0.988	0.633	0.672	0.352	0.255	0.470
August	0.989	0.782	0.769	0.704	0.264	0.589
September	0.992	0.783	0.804	0.860	0.343	0.744
October	0.997	0.859	0.887	0.945	0.789	0.786
November	1.003	1.163	1.136	1.160	1.617	0.937
December	1.049	1.430	1.480	1.280	2.894	1.295

Table A3c. Mean-monthly streamflow ratios for 3.0 ^{o}C T, 0% P

	Smith	Sacramento	Feather	American	Merced	Kings
January	1.252	1.780	2.081	1.754	5.023	1.908
February	1.163	1.565	1.830	1.687	3.874	1.872
March	1.133	1.412	1.543	1.595	2.964	2.242
April	1.135	1.055	0.949	1.154	1.753	2.049
May	1.163	0.635	0.462	0.545	0.901	1.169
June	1.144	0.528	0.453	0.335	0.584	0.701
July	1.083	0.730	0.762	0.428	0.393	0.633
August	1.096	0.899	0.881	0.807	0.378	0.729
September	1.192	0.914	0.926	1.006	0.550	0.889
October	1.314	1.098	1.097	1.370	1.250	0.933
November	1.357	1.605	1.610	1.737	2.668	1.328
December	1.317	1.911	2.018	1.767	4.037	1.851

Table A3d. Mean-monthly streamflow ratios for 3.0 ^{o}C T, 18% P

	Smith	Sacramento	Feather	American	Merced	Kings
January	1.038	1.535	1.755	1.430	6.372	2.008
February	0.968	1.323	1.517	1.402	4.804	2.163
March	0.944	1.108	1.187	1.208	3.156	2.679
April	0.959	0.750	0.602	0.816	1.233	1.756
May	0.980	0.389	0.256	0.266	0.370	0.585
June	0.988	0.380	0.334	0.182	0.139	0.288
July	0.988	0.595	0.626	0.322	0.088	0.285
August	0.989	0.742	0.716	0.671	0.111	0.478
September	0.992	0.751	0.756	0.825	0.153	0.652
October	0.997	0.838	0.856	0.925	0.718	0.698
November	1.003	1.246	1.160	1.224	2.012	0.925
December	1.051	1.612	1.597	1.344	4.277	1.689

Table A3e. Mean-monthly streamflow ratios for 5.0 ^{o}C T, 0% P

	Smith	Sacramento	Feather	American	Merced	Kings
January	1.390	2.243	2.639	2.211	9.455	3.079
February	1.285	1.879	2.173	2.065	6.726	3.019
March	1.257	1.542	1.712	1.792	4.283	3.634
April	1.251	1.017	0.868	1.154	1.781	2.434
May	1.288	0.529	0.333	0.400	0.582	0.897
June	1.242	0.472	0.411	0.268	0.286	0.443
July	1.146	0.715	0.753	0.406	0.165	0.416
August	1.166	0.907	0.873	0.809	0.204	0.581
September	1.332	0.954	0.936	1.057	0.381	0.769
October	1.565	1.240	1.198	1.672	1.497	0.844
November	1.605	2.069	2.022	2.324	4.415	1.629
December	1.497	2.521	2.622	2.243	7.343	2.978

Table A3f. Mean-monthly streamflow ratios for 5.0 ^{o}C T, 30% P

APPENDIX A4: GCM-forced Streamflow sensitivity values

	Smith	Sacramento	Feather	American	Merced	Kings
January	1.149	1.518	1.812	1.568	3.350	1.679
February	1.152	1.356	1.605	1.605	2.499	1.726
March	1.231	1.466	1.760	1.864	2.287	2.014
April	1.112	1.181	1.231	1.363	1.642	1.785
May	1.228	0.931	0.831	1.042	1.261	1.406
June	1.135	0.789	0.744	0.823	1.177	1.320
July	1.059	0.881	0.887	0.719	1.055	1.274
August	1.041	0.994	1.004	0.999	0.941	1.208
September	1.363	1.064	1.018	1.097	0.835	1.070
October	1.388	1.202	1.269	1.495	1.237	1.101
November	1.371	1.498	1.696	1.884	2.077	1.400
December	1.230	1.621	1.738	1.460	2.449	1.500

Table A4a. Mean-monthly streamflow ratios for HadCM2 2010-2039.

	Smith	Sacramento	Feather	American	Merced	Kings
January	1.269	1.794	2.227	1.893	4.965	2.055
February	1.238	1.550	1.916	1.836	3.601	1.982
March	1.350	1.642	1.989	2.269	2.960	2.665
April	0.956	1.059	1.117	1.248	1.863	2.137
May	1.095	0.785	0.674	0.863	1.212	1.411
June	1.062	0.654	0.603	0.634	1.057	1.226
July	1.016	0.805	0.847	0.578	0.830	1.116
August	0.951	0.933	0.966	0.933	0.710	1.092
September	0.984	0.915	0.988	1.076	0.709	1.040
October	1.672	1.388	1.365	1.628	1.252	1.066
November	1.243	1.475	1.700	1.874	3.045	1.668
December	1.427	2.064	2.277	2.003	4.467	2.352

Table A4b. Mean-monthly streamflow ratios for HadCM2 2050-2079.

	Smith	Sacramento	Feather	American	Merced	Kings
January	1.658	2.680	3.426	2.920	10.806	3.842
February	1.477	2.122	2.717	2.805	6.129	3.468
March	1.294	1.663	2.048	2.240	3.881	3.483
April	1.016	1.031	1.030	1.240	2.307	2.888
May	1.199	0.688	0.509	0.663	1.224	1.674
June	1.128	0.558	0.520	0.458	0.996	1.401
July	1.066	0.762	0.825	0.488	0.715	1.291
August	0.987	0.932	0.950	0.891	0.607	1.250
September	1.202	0.945	0.967	1.042	0.664	1.138
October	2.159	1.589	1.536	1.918	1.362	1.153
November	1.649	1.847	1.901	1.974	2.594	1.584
December	1.578	2.570	2.974	2.669	7.373	3.391

Table A4c. Mean-monthly streamflow ratios for HadCM2 2080-2099.

	Smith	Sacramento	Feather	American	Merced	Kings
January	0.814	0.793	0.853	0.816	1.092	0.978
February	0.981	0.966	1.032	1.052	1.231	1.080
March	0.991	0.977	0.980	0.974	1.167	0.972
April	1.007	0.981	0.952	0.983	1.054	1.054
May	1.068	0.919	0.886	0.919	0.931	0.937
June	0.907	0.875	0.906	0.940	0.964	0.924
July	0.986	0.927	0.883	0.946	0.910	0.906
August	0.911	0.920	0.929	0.964	0.881	0.903
September	0.895	0.907	0.923	0.978	0.835	0.925
October	0.650	0.750	0.850	0.860	1.077	0.927
November	0.819	0.908	0.969	0.995	1.378	1.082
December	0.865	0.851	0.907	0.891	1.179	1.048

Table A4d. Mean-monthly streamflow ratios for PCM 2010-2039.

	Smith	Sacramento	Feather	American	Merced	Kings
January	1.079	1.181	1.267	1.018	1.429	0.964
February	0.989	1.098	1.281	1.185	1.628	1.136
March	0.869	0.964	1.045	1.030	1.294	1.104
April	0.864	0.846	0.770	0.838	1.073	1.132
May	0.924	0.680	0.584	0.626	0.770	0.847
June	1.034	0.626	0.567	0.511	0.653	0.683
July	0.969	0.717	0.719	0.490	0.518	0.641
August	0.891	0.786	0.794	0.756	0.443	0.683
September	0.730	0.739	0.794	0.846	0.458	0.781
October	0.612	0.681	0.818	0.811	0.852	0.805
November	0.492	0.583	0.509	0.391	0.511	0.746
December	0.671	0.668	0.641	0.547	0.780	0.624

Table A4e. Mean-monthly streamflow ratios for PCM 2050-2079

	Smith	Sacramento	Feather	American	Merced	Kings
January	0.825	0.915	1.006	0.745	1.519	0.859
February	1.006	1.077	1.172	1.020	1.759	0.979
March	0.770	0.882	0.888	0.843	1.484	1.173
April	1.061	0.889	0.686	0.820	1.013	1.162
May	0.797	0.493	0.388	0.425	0.566	0.690
June	0.768	0.416	0.358	0.247	0.365	0.415
July	0.883	0.578	0.591	0.318	0.232	0.387
August	0.847	0.688	0.654	0.618	0.228	0.494
September	0.680	0.656	0.665	0.720	0.227	0.633
October	0.393	0.531	0.599	0.582	0.633	0.674
November	0.420	0.472	0.384	0.268	0.394	0.623
December	0.730	0.762	0.702	0.619	1.126	0.672

Table A4f. Mean-monthly streamflow ratios for PCM 2080-2099